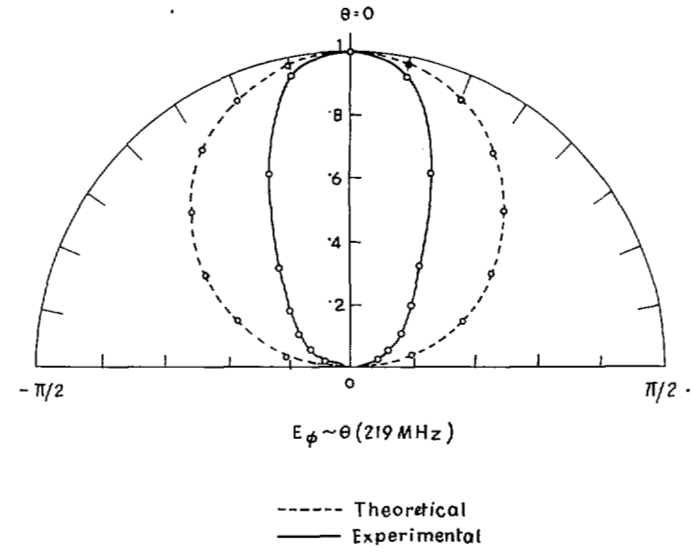


Fig. 4. $E_\phi$ versus $\theta$ radiation pattern of the microstrip antenna.

there are some differences in values. The method for theoretically calculating the distance of the feeding point from the open end for antenna matching to the feed line at resonant frequency also appears to be correct. Further reduction in size and increase in bandwidth could be expected with a proper choice of $w/h$ for which $\mu_{eff}$ has higher value.

## ACKNOWLEDGMENT

The authors wish to thank Professor J. S. Chatterjee for his guidance and encouragement.

## REFERENCES

[1] J. Q. Howell, "Microstrip antennas," *IEEE Trans. Antennas Propagat.*, vol. AP-23, pp. 90–93, Jan. 1975.
[2] E. Munson, "Conformal microstrip antenna and microstrip phased arrays," *IEEE Trans. Antennas Propagat.*, vol. AP-22, pp. 74–78, Jan. 1974.
[3] A. G. Derneryd, "Linearly polarized microstrip antennas," *IEEE Trans. Antennas Propagat.*, vol. AP-24, pp. 846–851, Nov. 1976.
[4] A. G. Derneryd and A. G. Lind, "Extended analysis of Rectangular microstrip resonator antennas," *IEEE Trans. Antennas Propagat.*, vol. AP-27, pp. 846–849, Nov. 1979.
[5] N. Das and S. K. Chowdhury, "Microstrip rectangular resonators on ferrimagnetic substrates," *Electron. Lett.*, vol. 16, pp. 817–818, Oct. 1980.
[6] A. D. Krall, J. M. McCorkle, F. John, and A. M. John, "The Omni microstrip antenna: A new small antenna," *IEEE Trans. Antennas Propagat.*, vol. AP-27, pp. 850–853, Nov. 1979.
[7] A. Robert Pucel and J. Daniel Masse, "Microstrip propagation on magnetic substrates-Part I: Design theory," *IEEE Trans. Microwave Theory Tech.*, vol. MTT-20, pp. 304–308, May 1972.
[8] M. V. Schneider, "Microstrip lines for microwave integrated circuits," *Bell Syst. Tech. J.*, vol. 48, pp. 1421–1444, May 1969.
[9] J. Watkins, "Radiation loss from open circuited dielectric resonators," *IEEE Trans. Microwave Theory Tech.*, vol. MTT-21, pp. 636–639, Oct. 1973.
[10] I. Wolff and N. Knoppik, "Rectangular and circular microstrip disk capacitors and resonators," *IEEE Trans. Microwave Theory Tech.*, vol. MTT-22, pp. 859, Oct. 1974.

# Tropospheric Wet Path-Delay Measurements

GUNNAR K. ELGERED

*Abstract*—**A dual-channel microwave radiometer measuring the sky brightness temperature at the frequencies 21.0 and 31.4 GHz, an infrared spectral hygrometer (IRSH) measuring the ratio of the radiation from the sun at the wavelengths 931 and 880 nm, and radiosondes have been used simultaneously to determine the excess path length due to water vapor (wet path delay) of radio waves propagating through the troposphere. By a least squares fit of the measured parameters from the microwave radiometer and the infrared spectral hygrometer, respectively, to the wet path delay calculated from the radiosonde profiles, the following root mean square (rms) differences of the wet path delay in the zenith direction were obtained: infrared spectral hygrometer–radiosondes, 1.1 cm; microwave radiometer–radiosondes, 0.7 cm; and 0.5 cm for a selected group of "good weather" data. The wet path delay was also calculated from surface meteorological measurements alone and the rms difference compared with corresponding radiosonde data was 2.0 cm in the zenith direction.**

## I. INTRODUCTION

It is important to have an accurate determination of the tropospheric path delay in many systems, e.g., at each antenna site during a radio interferometry experiment [1]. This delay can be divided into two components, a dry one and a wet one, and depends on the refractive index in the troposphere. The dry component–which is about 2.3 m in the zenith direction–is almost constant and its changes can easily be determined from ground measurements of pressure and temperature. The wet component, however, is dependent on the integrated amount of water vapor and varies from less than 1 cm to 20–30 cm in the zenith direction, depending on the climate and the local weather.

Reported here are measurements of the wet path delay only. For simplicity this component will from now on be called the delay. The results obtained with the different instruments and methods will be discussed in Section III. The instruments used are a microwave radiometer, called a water vapor radiometer (WVR), an infrared spectral hygrometer (IRSH), and radiosondes.

The WVR has been designed and built at the Onsala Space Observatory. The construction is described in [2]. The WVR measures the sky brightness temperature at the frequencies 21.0 and 31.4 GHz, the first close to the center of the water vapor line at 22.235 GHz and the other farther away from the line. The second frequency is necessary to deduce the effect of liquid water on the sky brightness temperature.

If the two measured sky brightness temperatures $T_{B,21}$ and $T_{B,31.4}$ are linearized, $T_{B,21}'$ and $T_{B,31.4}'$–to eliminate the saturation effect of $T_B$ for large atmospheric opacities–it is possible to obtain a linear expression for the delay $\Delta L$ of the following form:

$$\Delta L = a + bT_{B,21}' + cT_{B,31.4}' \quad (1)$$

Manuscript received February 26, 1981; revised May 4, 1981.
The author is with Chalmers Tekniska Högskola, Onsala Rymdobservatorium, S-439 00 Onsala, Sweden.

0018-926X/82/0500-0502$00.75 

where $a$, $b$, and $c$ are constants, depending mainly on the choice of frequencies but also to some extent on the meteorological profiles. However, an unsuitable choice of frequencies will make the constants more sensitive to changes in the meteorological profiles. For a detailed explanation of the theory, see Wu [3], and Moran and Penfield [4].

The IRSH was built at Meudon Observatory, France, and measures the ratio of the radiation from the sun at the wavelengths 931 and 880 mm. The atmospheric absorption in the infrared region is shown in [5]. When the IRSH is calibrated, the intensity ratio of the received radiation in the two frequency bands is a direct measure of the integrated amount of water vapor. Similar infrared instruments are described in [6] and [7].

The commercially available radiosondes used, manufactured by Vaisala Oy, Helsinki, Finland, measure the pressure, temperature, and relative humidity on their way up through the troposphere.

## II. MEASUREMENTS AND DATA REDUCTION

The observations reported here were carried out in May and June of 1980 at Gothenburg Airport, Sweden. Forty simultaneous measurements were made with the WVR and radiosondes, and 31 with the IRSH and radiosondes. Because the IRSH has to measure the radiation from the sun in clear weather, these observations had to continue until the middle of August, and for the same reason only seven simultaneous measurements were done with the WVR and the IRSH.

The wet part of the refractive index as a function of height was calculated from radiosonde profiles and then integrated to an altitude of approximately 9000 m to give the delay $\Delta L$, in centimeters, according to the formula (cf [8]),

$$\Delta L = 1.723 \cdot 10^{-3} \int_0^{\infty} \frac{a(h)}{T(h)}\, dh \tag{2}$$

where $a(h)$ is the water vapor density in grams/cubic meter; and $T(h)$ is the physical temperature in Kelvin.

The whole set of IRSH data was used to calibrate the IRSH against radiosondes. The intensity ratios, $V_1/V_2$ measured with the IRSH were fitted by means of the least squares method to the corresponding delay $\Delta L$, calculated from radiosonde data. The empirical formula

$$\Delta L = a e^{b V_1/V_2}, \tag{3}$$

where $a$ and $b$ are constants, showed good agreement with the data and was therefore used.

WVR data were taken twice a day, at noon and at midnight, when the radiosondes were launched. These data were then reduced with a technique similar to the one described by Claflin, Wu, and Resch [9], to give the sky brightness temperatures and then $\Delta L$ according to (1).

## III. RESULTS AND DISCUSSION

Results for two sets of data are presented. The first group represents all measurements and the second only "good weather" measurements, that is data taken when the clouds covered less than half the sky. During these conditions there is a smaller amount of heavy rain clouds than for all weather data. Rain and heavy rain clouds saturate the sky brightness temperatures and decrease the accuracy of the linearized temperatures. A small amount of clouds also indicates a more stable atmosphere. This is important for good agreement between WVR and radiosonde measurements, because the radiosonde needs about 25 min to reach an altitude of 9000 m.

In Figs. 1(a), 1(b), and 1(c) the delays in the zenith direction obtained from the radiosonde data are compared with those from surface meteorological measurements, the IRSH, and the WVR, respectively. All observations have been included. The root mean square (rms) differences of the calculated delays are shown in Table I.

The simplest method, which is, however, very inaccurate to predict the delay is to use the mean value for the season calculated from previous measurements. This method will, of course, give a higher error than the rms deviation of 3.2 cm obtained during these observations. The rms difference obtained when surface meteorological measurements are used is approximately the same as reported by Chao [10].

The improvement achieved when only good weather data are used instead of all data for the IRSH was less then 0.1 cm. This is expected because during severe weather conditions the sun does not break through the clouds during the radiosonde launching. Furthermore, we notice that the delays measured during the observations with the IRSH have a higher mean value than those for the WVR observations (cf Figs. 1(b) and 1(c)), which should be taken into account when we compare the accuracy between the IRSH and the WVR. When the 21 GHz sky brightness temperatures from the WVR are used alone, the rms difference in the least square fit with all data increases, mainly due to an average increase in the integrated amount of cloud liquid, compared with the good weather data where the accuracy is as good as for the dual-channel radiometer. The small improvement in the rms difference obtained with no constraint on $b$ and $c$—the constraint is given in Table I and will according to theory remove the influence of cloud liquid—in the formula $\Delta L = a + bT_{21}' + cT_{31}'$, shows that we have good agreement between the results and the theory. The rms difference obtained when the WVR data are compared with radiosonde data is surprisingly small. According to the radiosonde specification the radiosondes could be responsible for the whole difference. Furthermore, there probably exists an overestimation in the delay calculated from the radiosondes, due to a time lag constant in the hair hygrometer, which measures the relative humidity. This error will pass unnoticed through the least squares fit and then gives a corresponding overestimation in the derived coefficients.

The seven simultaneous measurements made with the WVR and the IRSH give a rms difference of 0.8 cm. If the errors of the instruments are not correlated, this implies that the WVR has the highest relative accuracy of the instruments used. However, because of the low number of simultaneous measurements this result should be treated just as an indication.

Finally, it should be pointed out that the absolute accuracy of the delay calculated from radiosonde data is not known. Therefore a systematic error in radiosonde data (e.g., the time lag constant in the hair hygrometer) will imply the same systematic error in the results from the WVR and the IRSH. Even if the absolute accuracy of the radiosonde were not known, there were two indications that the systematic error is

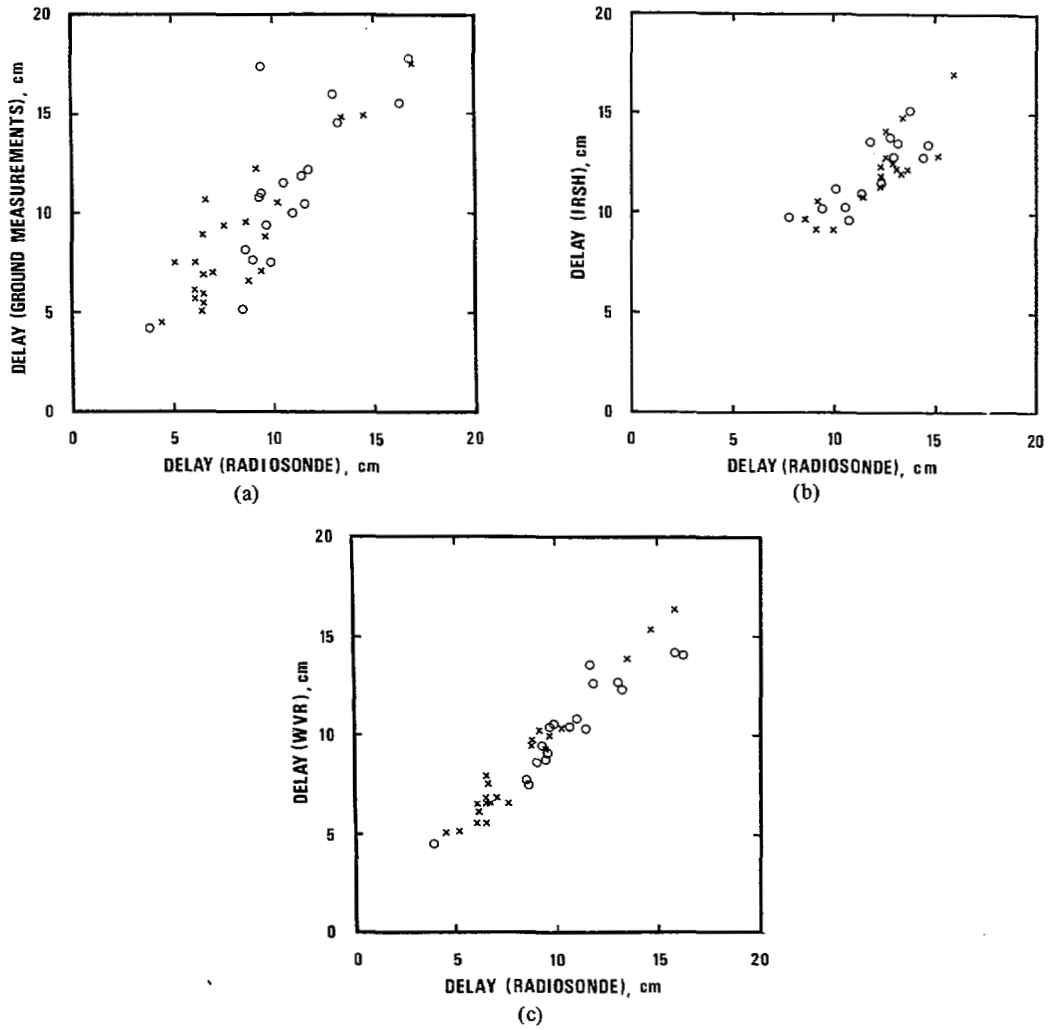


Fig. 1. Delay calculated from radiosonde data, in zenith direction, compared with delay obtained from (a) surface meteorological measurements, (b) IRSH observations, and (c) WVR observations according to the formula $\Delta L = a + bT_{21}' + cT_{31.4}'$ with the constraint on the coefficients $b$ anc $c$. The symbols denote: ($x$) good weather data (i.e., less than half the sky covered by clouds), and ($o$) remaining data (i.e., more than half the sky covered by clouds).

TABLE I
RMS DIFFERENCES OF THE WET PATH-DELAY IN THE ZENITH DIRECTION WHEN VARIOUS INSTRUMENTS AND METHODS ARE COMPARED WITH RADIOSONDE OBSERVATIONS

| Predictor | Fit(1) | rms Difference | |
|---|---|---|---|
| | | All data cm | Good weather data cm |
| Mean | No fit | 3.2(3) | 3.0(4) |
| Surface meteorological measurements | No fit(2) | 2.0(3) | 1.7(4) |
| IRSH | $\Delta L = ae^{bV_1/V_2}$(5) | 1.1(6) | 1.1(7) |
| WVR(8) | $\Delta L = a + bT_{21}'$ | 1.2(3) | 0.5(4) |
| WVR(8) | $\Delta L = a + bT_{21}' + cT_{31}'$ | 0.8(3) | 0.5(4) |
| with the constraint $c = -(21.0/31.4)^2 b$ | | | |
| WVR(8) | $\Delta L = a + bT_{21}' + cT_{31}'$ | 0.7(3) | 0.5(4) |

(1) $\Delta L$ calculated from radiosonde data.
(2) Calculation of $\Delta L$ as described by Chao [10].
(3) 40 data points.
(4) 22 data points.
(5) $V_1/V_2$ is the intensity ratio measured with the IRSH.
(6) 31 data points.
(7) 17 data points.
(8) The temperatures used are linearized as described by Wu [3].

rather small. 1) The mean value of the relative error between radiosonde and surface meteorological measurements, which are two independent methods, was 0.4 cm in the zenith direction. 2) When the sky brightness temperatures were calculated from radiosonde data (the theory is described in [11]), for measurements made during clear sky conditions, the mean of the relative error compared with the measured sky brightness temperatures was about 1 K for both channels. These mean relative errors correspond to an error in the delay of 0.5 cm in the zenith direction.

## IV. CONCLUSION

The measurements described show that the microwave radiometer has an accuracy comparable with the radiosonde to measure the excess path length caused by tropospheric water vapor. The microwave radiometer has to be calibrated against an independent instrument or method which has a low systematic error, but on the other hand, it is a simple instrument for continuous observations.

## ACKNOWLEDGMENT

The author wishes to thank the entire staff at the Onsala Space Observatory, in particular Prof. B. O. Rönnäng for continuous support during this work and for initiating the project, Mr. P. Lundh for his unfailing assistance at many occasions, Dr. J. I. H. Askne for helpful advice and stimulating discussions. He would also like to thank Dr. G. M. Resch at Jet Propulsion Laboratory, Pasadena, CA, for supplying useful information concerning the WVR technique. Dr. A. Greve at Max-Planck-Institut für Radioastronomie, Bonn, FRG for lending the IRSH, and the staff at the radiosonde station for their help during the observations. The construction of the WVR was financially supported by the Swedish Natural Science Research Council.

## REFERENCES

[1] I. I. Shapiro, "Estimation of astrometric and geodetic parameters," in *Methods of Experimental Physics*, vol. 12C, M. L. Meeks, Ed. New York: Academic, 1976, p. 264.

[2] G. Elgered, B. O. Rönnäng, and J. I. H. Askne, "*Remote sensing of atmospheric water vapor and cloud liquid*," Chalmers Univ. Tech., Onsala Space Observatory, Res. Rep. 141, 1980.

[3] S. C. Wu, "Optimum frequencies of a passive microwave radiometer for tropospheric path-length correction," *IEEE Trans. Antennas and Propagat.*, vol. AP-27, pp. 233–239, Mar. 1979.

[4] J. M. Moran and H. Penfield, "Test and evaluation of water vapor radiometers and determination of their capability to measure tropospheric path-length," NASA Contract Rep. NAS5-20975, 1976.

[5] C. W. Allen, *Astrophysical Quantities*. London: Athlone, 3rd ed. 1973, pp. 128–130.

[6] S. Sivertsen and J. E. Solheim, "A field instrument for water vapour measurements," *Infrared Phys.*, vol. 5, pp. 79–82, 1975.

[7] E. Bücher and D. Lemke, "An infrared hygrometer for astronomical site testing," *Infrared Phys.*, vol. 20, pp. 321–325, 1980.

[8] E. K. Smith and S. Weintraub, "The constants in the equation for atmospheric refractive index at radio frequencies," *Proc. I.R.E.*, pp. 1035–1037, Aug. 1953.

[9] E. S. Claflin, S. C. Wu, and G. M. Resch, "Microwave radiometer measurement of water vapor path-delay: Data reduction techniques," *Report 42-48*, Jet Propulsion Lab., Pasadena, CA, DSN progress Rep. 42-48, pp. 22–30, Sept.–Oct. 1978.

[10] C. C. Chao, "A new method to predict wet zenith range correction from surface measurements," Jet Propulsion Lab., Pasadena, CA, Tech. Rep. 32-1526, vol. XIV, Apr. 15, 1973.

[11] J. W. Waters, "Absorption and emission by atmospheric gases," in *Methods of Experimental Physics*, vol. 12B, M. L. Meeks, Ed. New York: Academic, 1976.

# Trapped Image Guide Leaky-Wave Antennas for Millimeter Wave Applications

TATSUO ITOH, FELLOW, IEEE, AND BERND ADELSECK

***Abstract*—A leaky-wave antenna is developed from a novel dielectric waveguide for millimeter wave applications. Design formulas and data are provided, and measured and computed results are presented for a prototype model.**

## I. INTRODUCTION

Recently, several investigators have reported on the grating-type leaky-wave antennas created for millimeter wave integrated circuits [1]–[3]. The one created in the inverted strip dielectric waveguide [4] can be made conformable with a built-in radome [1]. This waveguide, however, is relatively weakly guiding and it is also difficult to suppress the unwanted radiation at the curves and bends in the radio frequency (RF) front end connected to the antenna, though the latter performed quite well. The antennas created on an image guide are not flush mounted as the image guide has a structure made of a dielectric rod on a ground plane. The proposed antenna in this communication circumvents these difficulties. It can be flush-mounted and is made of an open dielectric waveguide in which unwanted radiations at bends are considerably reduced.

This communication describes the design and test operation of a leaky-wave antenna made of a novel dielectric waveguide developed for millimeter wave integrated circuits. Some of the features of this antenna are: 1) since the operation is based on the grating coupler in integrated optics, this antenna becomes more attractive at higher frequencies; 2) it is frequency-scannable over a wide sector; 3) it can be flush-mounted and is conformable; and 4) it can be integrated with the rest of RF front end of the millimeter wave circuits.

## II. ANTENNA STRUCTURE

The basic building block of the antenna is a novel dielectric waveguide called the trapped image guide [5], the cross section of which is shown in Fig. 1. This is basically an image guide with two side walls of finite height $h$. By choosing an appropriate value of $c$ for given values of $\epsilon_r$, $a$, and $b$, we can get a waveguide in which the propagation constant $k_z$ is pratically identical to the one for a conventional image guide ($c \to \infty$) except at extremely low frequencies. However, when this waveguide is bent in the sideward direction, the radiation loss is typically reduced by more than 6 dB per a 90° bend of radius 63.7 mm as compared to the image guide setup [5].

A breadboard model of a leaky-wave antenna setup for a *Ka*-band operation is shown in Fig. 2. The center portion of the structure is the antenna consisting of a metal strip grating placed on the dielectric rod of the trapped image guide. The trapped image guide itself was created by adding

Manuscript received July 8, 1980; revised April 14, 1980 and June 2, 1981. This work was supported in part by the U.S. Army Research Office under Grant DAAG29-78-G-0145.

T. Itoh is with the Department of Electrical Engineering, University of Texas, P. O. Box 7728, Austin, TX 78712.

B. Adelseck is with the Hochfrequenztechnik, AEG-Telefunken, D-7900, Ulm, West Germany.

0018-926X/82/0500-0000$00.75 